Creep Response of Various Solders used in Soldering Ball Grid Array (BGA) on Printed Circuit Board (PCB)

Joshua A. Depiver, *Member, IAENG,* Sabuj Mallik and Emeka H. Amalu

***Abstract*—In electronics packaging, solder joints play a critical role by providing electrical, thermal and mechanical connections between the package and the printed circuit board (PCB). As the joint is both miniature and brittle, it is the weakest part of the assembly and thus susceptible to untimely damage. This paper presents the creep response of solder joints in a ball grid array (BGA) soldered on a PCB subjected to isothermal ageing in one experiment and temperature cycling in another test. The ageing is simulated in an ANSYS package environment at -40, 25, 75 and 150°C temperatures applied for 45 days. The thermal cycling profile started from 22°C and cycled between -40°C and 150°C with 15 minutes dwell time at the lowest and highest temperatures. The solders used in the investigation are lead-based eutectic solder alloy and lead-free SAC305, SAC387, and SAC396 solders. The research seeks to qualify these solders against strain and strain energy response for improved reliability in operation. The results show that the lead-free SAC387 accumulated the maximum strain and thus strain energy while the lead-based eutectic solder is found to accrue the least amount of the quantities. Further results show the distribution of damage in the BGA solder bump. Based on the results, it is proposed that lead-free SAC396 is the best replacement of the lead-based eutectic solder in the drive for the achievement of comparable thermo-mechanical reliability of assembled BGA on PCB.**

***Index Terms*—Creep Strain, Strain Energy, Ball Grid Array (BGA), Thermal Cycling, Isothermal Ageing**

I. Introduction

IN In electronic devices, solder joint reliability has grown to be very vital for the operational performance of electronics systems used in safety-critical applications such as aeroplane, defence, oil and gas drilling applications, automobile, medical devices, and power grids. Because solder joints are applied at high temperatures and small, their reliability is of fundamental interest to electronics manufacturing engineers and industries. The capability of solder joints to remain in conformance with their mechanical, electrical and visual specifications over a specified duration, under a specific set of operational provisions is referred to as solder joint reliability. Reliability of these joints is determined by multiple factors such as shear strength, creep resistance, drop shock, thermal fatigue and vibration resistance. Due to the adoption of the Restriction of Hazardous Substances (RoHS) directives on July 1, 2006, by the European Union (EU), there have been new progress and developments in lead-free solders as a replacement for the conventional lead-based solders for application in the electronics manufacturing industries [1-5]. Amongst the lead-free solders investigated, Sn-Ag and Sn-Ag-Cu based solders offer the most promising characteristics as replacement of lead-based solders [6-7]. Introduction of new lead-free solders added a new dimension to reliability issues in electronic devices. Solder joints provide the essential mechanical, electrical and thermal connections between package elements and substrate in electronics packaging.

These joints moreover serve as the weakest links in the overall package in the sense that if any of these joints fail, then the entire system could eventually fail and stop functioning. From a structural point of view, solder joints are heterogeneous and dynamic systems. It is significant to examine several elements of the solder structure, to know their thermo-mechanical behaviours. While in operation, electronic products are exposed to a variety of application conditions such as vibration, which can induce impact and fatigue failures. Thermal ageing of solder joints, on the other hand, produces changes in solder microstructure and could trigger creep failure [8-9]. Knowledge and understanding of the failure of these systems are essential to preventing accidents [10]. The cyclical variation of thermal stress produces solder joint thermal fatigue failure. Throughout thermal cycling, creep is the primary tool of thermal deformation fatigue failure. With ambient temperature changes (e.g. temperature periodicity rises and fall) or component emits heat (e.g. systematic power on and off), solder joints will generate thermal stress. The cyclical change of thermal stress influences the solder joint thermal fatigue failure. In the course of thermal cycling, creep is the primary process of thermal deformation fatigue failure [11].

II. Solder Alloy Creep Model

Solder alloys are considerably used in all electronic packaging as a result of their low melting temperature and excellent wetting properties. However, in most electronic packaging, solder alloys function at the thermally activated condition at room temperature, as a result of their low melting point. Packaging in electronics equipment comprises materials with very different mechanical and thermal properties. In service, discrepancies of CTE of various materials produces cycling shear stress on solder joints. The

Manuscript received July 30, 2019; This work was supported by The University of Derby

Joshua Depiver is a PhD researcher in the Department of Mechanical Engineering & Built Environment, College of Engineering & Technology, University of Derby, Markeaton Street, Derby, DE22 3AW, United Kingdom e-mail: j.depiver@derby.ac.uk., Telephone: +44 794 467 6697

Dr Sabuj Mallik is an associate Professor in the Department of Mechanical Engineering & Built Environment, University of Derby, Markeaton Street, Derby, DE22 3AW, United Kingdom, e-mail: s.mallik@derby.ac.uk.

Dr Emeka H. Amalu is a senior lecturer in the Department of Engineering, School of Science, Engineering and Design, Teeside University, Middlesbrough TS1 3BA, United Kingdom, email: e.amalu@tees.ac.uk.

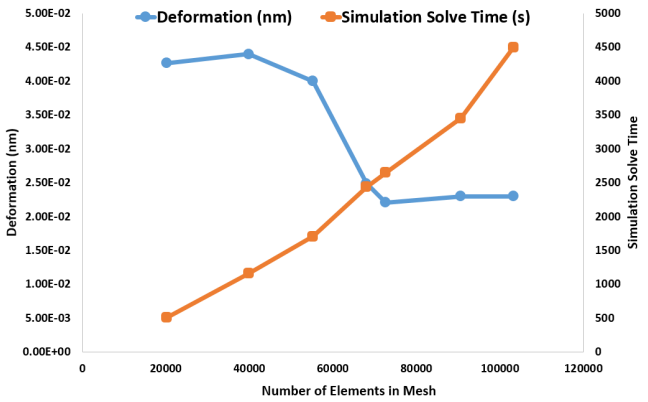

Fig. 1. **P**lot of Convergence versus Simulation time for SAC305 model

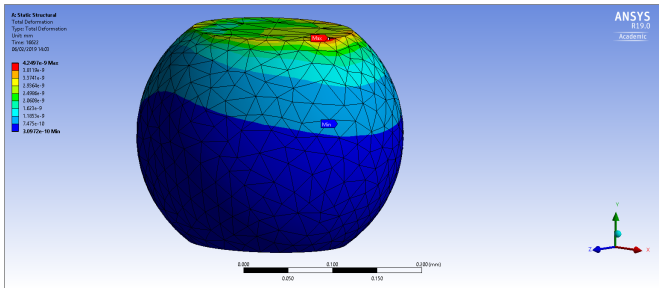

Fig. 2. **S**imulated result for Total Deformation of SAC305 of sub-modelled solder

stresses build fatigue failure of solder joints, and fatigue life of solder joints typically determines the reliability of electronic packaging. Fairly a limited number of investigators developed creep models for viscoplastic behaviours of solder joints. Basaran et al. (2005) [12] and Gomez and Basaran (2006) [13] have identified these references on constitutive modelling of solder alloys. The analyses have shown that the creep behaviour of a solder alloy significantly depends on age, stress, temperature, and grain size. However, a full review and an evaluation of these models have never been published. Ghorbani and Spelt (2007) [14] developed the thermo-mechanical models of solder joints so that test data and life prediction can be based on the stress-strain response of the solder. The projections of the present model correlate well with the experimentally measured number of cycles-to-failure using the Coffin-Manson strain-based model [15-16] for the SnPb solder and energy-based life prediction model for the SAC solder joints.

III. Accelerated Thermal Cycling Test

A. *Finite Element Modelling & Analysis*

1) Convergence and Mesh Independence Study

It does not take much for an FEA to produce results. However, for results to be accurate, we must demonstrate that results converge to a solution and are independent of the mesh size. A mesh convergence study establishes that the FEA model has converged to a solution. It also justifies mesh independence and additional refinement is unnecessary. The results of an FEA model must be independent of the mesh size. The initial results obtained from meshing the whole components are shown in Fig. 1-2. A convergence study ensures that the FEA model captures the behaviour of the system while reducing solve time. It shows a very fine optimised sub-modelled mesh from convergence mesh study with the convergence and mesh independence data. The convergence results in mesh refinement are shown in Fig. 1 for the convergence versus simulation solves time (seconds) for lead-free SAC305 solder. The simulation result presented in Fig. 2 indicates the area of total deformation at the BGA of the model. A fine mesh is used in the region of high-stress gradients, and coarse mesh is ignored. It can be seen from Fig. 1 that the more the mesh becomes finer, it does require considerably high CPU simulation solve time.

Lead-free solder materials are susceptible to significant creep deformations in harsh high-temperature environments such as oil exploration, automotive, avionics, and military applications. Also, degradations will happen in the creep responses of lead-free solder alloys when they are exposed to long-term isothermal ageing during product applications at high temperatures. Fahim et al. (2016) [15] examined high temperature creep response of lead-free solders. In their work, they characterised the high temperature creep behaviours of SAC405 and concluded that SAC alloys were more resistant to creep at high temperature. Several studies have investigated creep such as Ma, et al. (2006/2007) [16-17], Zhang, et al.(2008/2009) [18-19], Cai, et al. (2010) [20], Zhang, et al. (2013) [21], Zhu, et al. (2015) [22] and Amalu & Ekere, (2016) [23]. Creep deformation has become a dominant deformation in electronics devices and happens when $T_H = T\backslash T_m$ go above 0.4 and also occurs at fairly low temperatures [24-25].

Otiaba et al. (2013) [26] investigated FEA of the effect of silver content for SnAgCu alloy compositions on thermal cycling reliability of solder die to attach. Their study suggests that the range of stress was relatively more significant for the SAC alloy with higher Ag content (SAC405) while the lower Ag content SAC solder (SAC305) experiences a comparatively larger accumulated plastic work under the same thermal cycling condition. The optimal silver (Ag) content in the SnAgCu alloys is crucial in fabricating a Solder Thermal-Interface Material (STIM) that relatively has an improved thermal fatigue performance as reported by Terashima et al. (2003) [27]. They investigated the thermal fatigue properties of Sn-xAg-0.5Cu (x = 1, 2, 3, and 4 in mass %) flip-chip interconnects to study the effect of silver (Ag) content on thermal fatigue endurance. The research concluded that solder joints with lower silver context (x = 1 and 2) had a greater failure rate compared to those with higher silver content (x = 3 and 4) in thermal fatigue testing. Mustafa et al., 2011 reported on the effect of solder composition for four SAC alloys; Sn1Ag0.5Cu (SAC105), Sn2Ag0.5Cu (SAC205), Sn3Ag0.5Cu (SAC305) and Sn4Ag0.5Cu (SAC405)) with different silver content (1-4%) under strain-controlled cycling. They also performed cyclic testing on the effect of temperature on SAC samples at four different temperatures (25, 50, 75 and 100°C). Before cyclic loading, the specimens in their study were aged (preconditioned) at 125°C for various ageing times (0-6 months).

2) Creep Parameters and Constitutive Relationship of Lead-Based Eutectic Solder and Lead-Free SAC Solders

The thermo-mechanical response of the solder joint is very vital in the design of a reliable electronics circuit board assemblies, and creep plays an essential role in the damage mechanism of solder joints. Under different operating conditions, solder joints experience several categories of loading conditions, which include thermal cycling, vibration and shock, over-stress, and cycle bending of circuit boards. As a result of every loading condition, solder may creep or rupture. Creep are considered as the principal deformation mechanisms in the solder joints [28] and are examined critically in this section. Several creep constitutive model has been reported. The Garofalo-Arrhenius constitutive relation has been adopted for this research because its usage has an outstanding capability of improving the accuracy of prediction of the magnitude of damage in solder joints [29-30].

3) Garofalo-Arrhenius Creep Theory

When a material is applied at constant stress and the strain increases with an increase in time, this is referred to as creep effect. In other words, creep is a time-dependent deformation. Creep effect is more critical in metallic material at high homogeneous temperature. Amalu & Ekere (2016) [23] investigated the modelling evaluation of Garofalo-Arrhenius creep relation for lead-free solder joints in surface mount electronic component assemblies. They used different creep parameters in Garofalo-Arrhenius constitutive creep relation and used four set of values, proposed by Lau (2003) [31], Pang et al. (2004) [32], Schubert et al. (2003) [33] and Zhang et al. (2003) [34], to generate four hyperbolic sine creep relations and proposed a paradigm for selecting suitable constitutive model(s) for accurate prediction whilst suggesting the development of new solder constitutive relations. The Garofalo creep constitutive constants used are shown in Table V. The implicit model of ANSYS R19.0 for solders obeying Garofalo Arrhenius creep constitutive equation works very well and converges very fast.

Ramachandran & Chiang (2017) [35] investigated the feasibility evaluation of creep model for failure assessment of solder joint reliability of wafer-level packaging. They developed a new creep model based on the assumptions that an instantaneous steady-state creep form eliminates the evolution term, resulting in a creep equation with four parameters and the proposed model has a similar vital statement similar to that of the well-known hyperbolic sine model. The model considerably broadens the application of the hyperbolic model. They used a WLCSP on PCB and performed thermal cycling experiments in ESPEC TCC-150. The steady-state creep is the dominant deformation experienced by solder alloys. This can be quantitatively estimated, and a series of constitutive models were proposed. The two models that are widely accepted for the characterisation of solder alloys by considering the diffusion-controlled creep deformation mechanism [36]:

Dorn Power Law [37]

$$\varepsilon = A\sigma^n exp\left(\frac{-Q}{RT}\right) \tag{1}$$

Garofalo Hyperbolic Sine Law [38]

$$\dot{\varepsilon} = A\left[\sinh\left(\alpha\sigma\right)\right]^n e^{(-Q/RT)} \tag{2}$$

Where $\dot{\varepsilon}$ is creep strain rate, A (C_1) is a material constant, α (C_2) is a multiplier of hyperbolic-sine law, which is obtained from curve fitting to experimental data by using linear and nonlinear least square regression, ρ is the applied shear stress, n (C_3) is the stress exponent which can be determined from creep deformation map, it can be found that the deformation mechanism is dislocation creep, so n is between 5 and 7. Q (C_4) is the activation energy, R is the universal gas constant, and T is the temperature in Kevin. The models show that the steady-state creep strain rates are strongly stressed and temperature dependent.

4) Basic assumptions and analysis methodology:

- The material property of the solder bump is nonlinear and temperature-dependent. In other words, others are linear and temperature-independent.
- Process variations were not considered, and IMC growth was ignored.
- Every interface of the materials is assumed to be in contact with each other.
- All the materials were modelled as linear elastic and isotropic materials except the solder and PCB which are simulated using the Garofalo creep relations and orthographic materials respectively.
- All materials including the solder joint were assumed homogeneous at load steps
- The assemblies were assumed to be a stress-free state at room temperature of $22^{\circ}\mathrm{C}$ which was also the starting temperature of the thermal cycle loading.
- The initial stress in the assemblies which may be accumulated from the reflow soldering process is neglected, and all contacting surfaces are assumed to be bonded with perfect adhesion.

5) Geometrical and Mesh Models

The BGA package includes Silicon (Si) Die Substrate, Solder Ball, Epoxy-Resin (FR-4) and Copper Pad. The parameters and package dimensions of the lead-free solder BGA are shown in Table I & II:

The full model and the mesh FE model, along with the optimised mesh of the assembled components used for the ANSYS simulation, are shown in Fig. 3 (a). Similarly, the quarter view of the assembled component is shown in Fig. 3 (b).

6) Finite Element Model and Methodology

A 3D FE model of the assembly of the BGA and PCB components is shown in Fig. 3 which was created using a combined construction geometry (SolidWorks). The FE model was input into ANSYS software R.19.0 FEM software where their static structural response to cyclic induced thermal loads was simulated. The default mesh was not used for the simulation process. This was because the symmetry of the structure was not harnessed; therefore, the shape of the solder balls after generating a mesh looks deformed, consequently getting the correct and adequate simulated result will be inhibited. The meshed components part of the solder balls undergoes convergence study in

TABLE I
PARAMETERS OF LEAD-FREE BGA SOLDER ARCHITECTURE

Balls	Ball Matrix	Pitch (mm)	Size (mm)	Substrates	Part Number	Reference	Quick View
36	6x6	0.5	3.0	Silicon (Si)	WLP36T.5C-DC067D	TopLine (2016) [39]	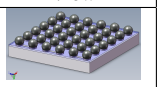

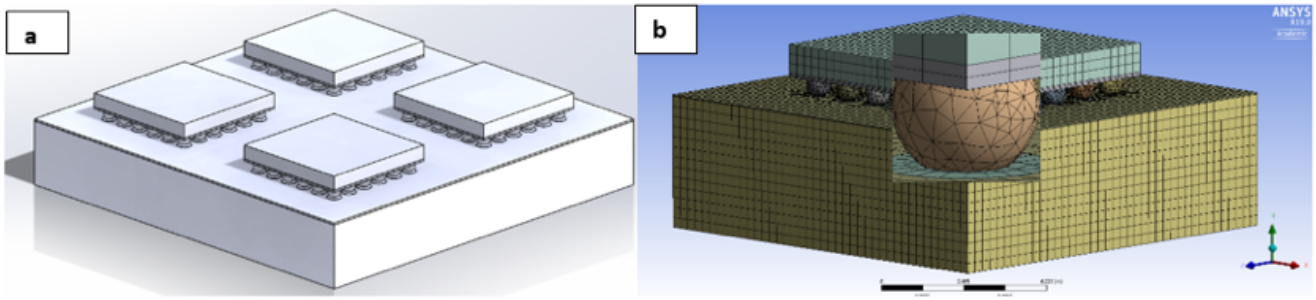

Fig. 3. (a) Full Model of assembly (b) A quarter assembly of the modelled lead-free BGA assembled on a PCB using the solder joints as the interconnection technology (assembled components)

TABLE II
PACKAGE DIMENSIONS

Package	Dimensions (mm where applicable)
PCB	5x5x1.6
Solder Mask Thickness	0.05
Substrate (Silicon)	3x3x0.35
Cu Pad Diameter	0.36
Cup Pad Thickness	0.02
Die (Epoxy-Resin)	5x5x0.05
Solder Ball Height	0.24
Solder Balls	36
PCB Mask	0.05

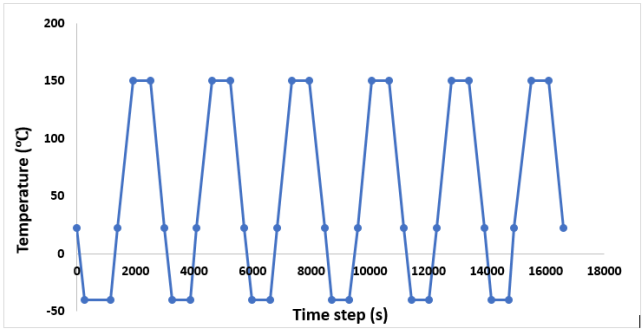

Fig. 4. **T**emperature boundary conditions

order to arrive at a converged solution and mesh independent.

7) Material Properties and Parameters

Except for the PCB, the properties of all other materials are considered to be linear and temperature-dependent. The material properties used are obtained from several works of literature. The critical materials used in the assembly in mounting the BGA on PCB are: SAC solder alloys, Copper Pad, Epoxy-Resin (FR-4), Solder mask and Silicon (Si) die. The components assembled does not contain the Intermetallic compounds (IMC) because the effect is assumed not to have any influence on the research outcomes. All the materials were modelled as linear elastic and isotropic substances except the PCB and the solder alloys, which was simulated using the orthographic materials and Garofalo creep relations respectively. The materials properties are shown in Table III, and the composition of leaD-based eutectic and lead-free SAC solders test samples are shown in Table IV.

8) Loading and Boundary Conditions

In performing the FE Analysis, the ambient temperature cycle is external loading. The FE models were subjected to six complete ATCs in 36 steps shown in Fig. 4. The thermal cycling temperature from $-40°C$ to $+150°C$ with 15°C/min ramp and 600s dwell based on IEC 60749-25 temperature cycling and JEDEC Standard JESD22-A104D [40-41] was used. The quarter assembly components were first heated from room temperature $22°C$, which is the starting temperature in thermal cycle loading with constant heating rate. They are also assumed to be at a homologous temperature at loads steps. The temperature loading started from 22°C, dwelled at $-40°C$ at the rate of 15°C/min, and ramped up to $22°C$ for 1,380s and excursion temperature (ET) of $150°C$ for 1,908s where it dwelled for 600s. The composition of lead-free SAC alloys and lead-based eutectic solder are shown in Table IV. The temperature was assumed to be $150°C$ to obtain final results. Devices for this profile are the automotive applications and for semiconductors in power supply controllers. They also account for the full range of temperature cycle for military applications. The assemblies were supported such that the conditions of the structure at the supports are:

At the PCB base, $y = 0$, and u_y = 0; Top surface u_y = 0, u_x and u_z are free. The u_x, u_y and u_z represents the displacement in the x,y and z directions respectively. The bottom surface of the PCB was fixed in Y direction and displaced in the X and Z directions.

Several research, including one by Ma et al. (2006) [43] has established how the creep resistance of SAC solders decreases with an increase in time and temperature during

TABLE III
THERMO-ELASTIC MECHANICAL PROPERTIES OF MATERIALS OF BGA ASSEMBLIES

S/No	Materials	Reference	Young's Modulus (GPa)			C.T.E (ppp\°C)			Poisson's Ratio			Shear Modulus (GPa)		
			E_x	E_y	E_z	σ_x	σ_y	σ_z	v_{xy}	v_{xz}	v_{yz}	G_{xy}	G_{xz}	G_{yz}
1	Silicon (Si) Die	TopLine (2016) [39]	110.0			2.60			0.24			50.8		
2	PCB Mask	Zahn (2002) [65]	4.14			30.0			0.40			1.48		
3	Cu Pad	T.Nguyen, et al. (2010) [66]	129.0			17.0			0.34			48.1		
4	PCB	Amalu & Ekere (2016) [23, 71]	27.0	27.0	22.0	14.0	14.0	15.0	0.17	0.20	0.17	27.0	22.0	27.0
5	Epoxy-Resin (FR-4)	TopLine (2016) [94]	29.9	25.1	70.0	12.0	15.0		0.16	0.14		12.9		
6	Sn63Pb37	Long, et al. (2018) [67]	56.0			20.0			0.30			21.5		
7	SAC305	TopLine (2016) [39]	51.0			23.5			0.40			18.8		
8	SAC387	Beyer, et al. (2016) [68]	32.0			64.0			0.36			16.5		
9	SAC405	J.Eckermann, et al. (2014) [69]	44.6			20.0			0.42			15.7		
10	SAC396	Stoyanov, et al. (2009) [70]	43.0			23.2			0.30			16.5		

TABLE IV
COMPOSITION OF LEAD-BASED EUTECTIC AND LEAD-FREE SAC SOLDERS TEST SAMPLES

Sample	SAC Alloys	Composition	Reference	Notes
1	SAC305	Sn-3.0Ag-0.5Cu	Almit Ltd (2005) [42]	JEITA (Japan)
2	SAC387	Sn-3.8Ag-0.7Cu	Ma & Suhling (2009) [44]	EU
3	SAC405	Sn-4.0Ag-0.5Cu	Ma & Suhling (2009) [44]	Global
4	SAC396	Sn-3.9Ag-0.6Cu	Almit Ltd (2005) [42]	iNEMI (USA)
5	N/A	63Sn-37Pb	Ma & Suhling (2009) [44]	Eutectic (Standard)

TABLE V
CREEP CONSTITUTIVE CONSTANTS FOR SOLDER ALLOYS

Constitutive Model	Solder Alloy	Reference	$C_1(s^{-1})$	C_2	$C_3(MPa)^{-1}$	$C_4(KJ/mol)$
Garofalo Sine Hyperbolic	Sn63Pb37	Wiese et al. (2001) [45]	10	0.1	2.0	44.9
	SAC305	Vianco (2006) [46]	2630	0.0453	5.0	52.4
	SAC387	Schubert et al. (2005) [33]	32000	0.037	5,1	65.3
	SAC405	Wang et al. (2005) [47]	17	0.14	4.2	55.0
	SAC396	Lau et al. (2003) [31]	441000	0.005	4.2	45.0

isothermal ageing. They reviewed a full effect of ageing on the creep behaviour of lead-free solders with particular focus on SAC305 and SAC405. They also conducted other investigative experiments for varying temperature duration from 3-63 days at room temperature. Ma et al. (2009) [44] also studied the influence of elevated temperature ageing on the reliability of lead-free solder joints. The researchers mentioned that the lead-free and eutectic samples were aged at various intervals from 0-6 months at several elevated temperatures (80,100,125 and 150°C). Analogous creep test was performed with the eutectic solder sample (63Sn-37Pb) for evaluation and validation of results purposes.

IV. ISOTHERMAL AGEING OF SOLDER JOINT

The influence of thermal ageing on the evolution of the solder joint cannot be underestimated. The behaviour of lead-free solder joints in electronics assemblies is continually evolving when exposed to isothermal ageing and thermal cycling environments. The study has investigated both phenomena during the short and long term ageing of solder joint in harsh environments. For this research, we have considered creep test temperature of -40°C, 25°C, 75°C and 150°C for 45 days of ageing test experimentally.

The work carried out by Sabbah, et al. (2017) [48] studied the high-temperature ageing of microelectronics assemblies with SAC solder joints. They investigated the failure mechanism and microstructure evolution of lead-free solder joints at a maximum temperature of 175°C. It is found that no new failure mechanisms are triggered and that ageing tests for solder can be accelerated at 175°C. In particular, the growth rate of the interfacial IMC is found to be consistent with that observed at lower temperatures. In conclusion, it was found that the joints degrade rapidly, especially in cycling conditions. However, the ageing tests performed at 175°C did not show any new failure mechanism compared to previous results obtained at lower temperatures. Therefore, it is possible to run ageing tests at 175°C on lead-free SAC soldered assemblies to perform a faster reliability assessment. Moreover, the estimated value of the activation energy indicates that mass transport controlled through grain boundary diffusion is crucial for Pb-rich coarsening under

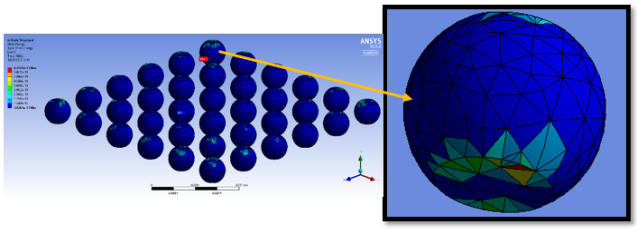

Fig. 5. Strain energy result for SAC305 solder subjected to thermal cycling

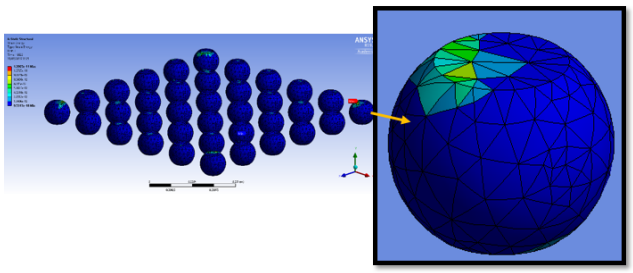

Fig. 6. Strain energy result for SAC396 solder subjected to thermal cycling

ageing treatment. For the research investigations, the BGA on the PCB model was simulated using the properties of the material in Table III for the lead-free SAC and lead-based eutectic solders applied for a period of 45 days (64,800s). It could be observed that cracks/ruptures are taught to develop around the solder balls flanges. These results indicate that these areas require maximum reliability attention.

V. RESULTS AND DISCUSSIONS

A. Isothermal Ageing of Solder Joint

The simulated results obtained using the thermo-elastic mechanical properties implemented in the global calculations for an isothermal ageing effect shows areas of high deformation. A constant temperature of -40°C, 25°C, 75°Cand 150°C was used for the simulation studies. From the results, it was found that creep deformation tends to occur at a significant rate when the homologous temperature is 0.4 or higher. From the homologous temperatures obtained from calculation, it was observed that all lead-based eutectic and lead-free SAC solders have higher homologous temperature as for eutectic (0.50, 0.65, 0.76 & 0.93), SAC305 (0.46, 0.60, 0.71 & 0.86), SAC405 (0.47, 0.61, 0.71 & 0.86), SAC387 (0.46, 0.61, 0.71, & 0.86) and SAC396 (0.46, 0.60, 0.70 & 0.86). It is also ascertained that creep occurs faster at higher temperatures. However, what constitutes a high temperature is different in different SAC solders. As stress increases, the rate of deformation increases.

B. Thermal Cycling of Solder Joint Interconnect

1) Strain energy simulation results for solder joint subjected to thermal cycling

The strain energy results are shown in Fig. 5-9 tend to show a good relationship between the experimental (from literature) and simulated (numerical) strain energy. The strain energy results would suggest that creep and strain continue to play a significant role in solder joint creep-fatigue even under conditions that would tend to be extended beyond typical low-cycle thermal cycling used in this work. Just like the creep deformation results, we observed similar outcomes with SAC387 having higher strain energy in comparison with the lowest strain energy of lead-based eutectic solder, as shown in Fig. 9. At higher power cycles, the strain energy-based model is capable of relatively accurate prediction with our dwell time of less than 15 minutes. This is true even for conditions that extended beyond low-cycle thermal cycling.

The graph of the damage distribution and strain energy for lead-based eutectic and lead-free SAC solders is shown in Fig. 9. From the plot, we could deduce that the magnitude of the creep strain varies for different solder alloys used.

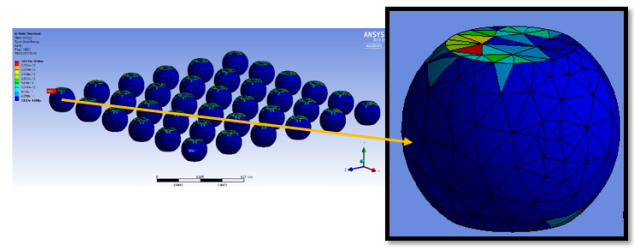

Fig. 7. Strain energy result for SAC387 solder subjected to thermal cycling

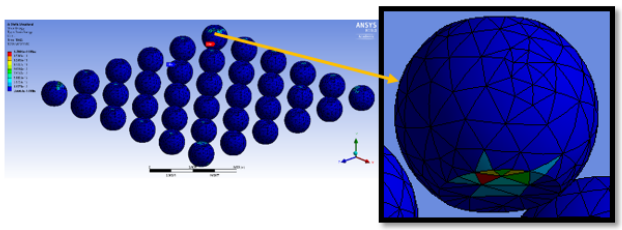

Fig. 8. Strain energy result for lead-based eutectic solder subjected to thermal cycling

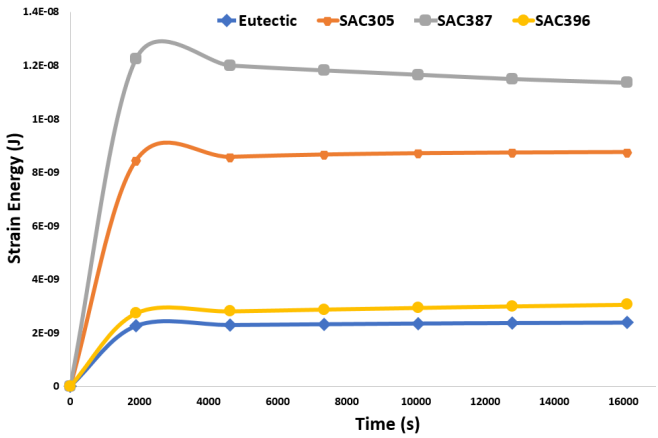

Fig. 9. Strain energy plots for lead-based eutectic and lead-free SAC solders subjected to thermal cycling

Dasgupta & Oyan (1991) [50] analysed a specimen solder to obtain the inelastic strain history during two different temperature cycles specified by UNISYS. As we have modelled the creep behaviour with Garofalo, the strain rate is assumed to have a power-law dependence on the stress magnitude. It is evident that when the temperature is large, the strain components increases and the maximum strain concentration with a move to the diagonal edges of the solder interface and fails due to creep cracks propagation

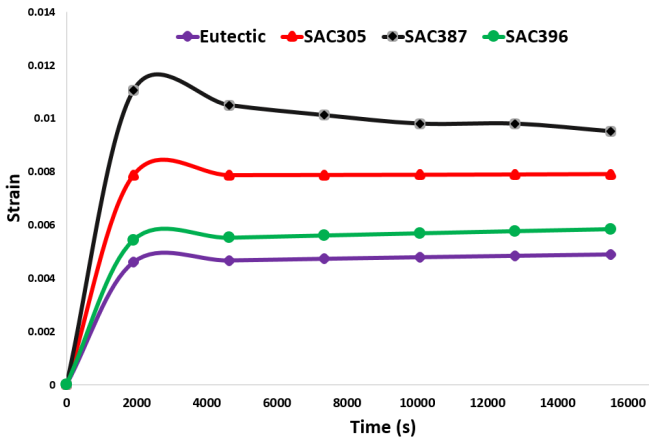

Fig. 10. **T**he strain-time curve for lead-based eutectic and lead-free SAC solders subjected to thermal cycling

and rupture. The element sizes vary from 0.01 to 0.005 and show the transformation from coarse mesh to very fine mesh until when two or three meshes have the same result. It is observed that the trend of the deformed portion of the solder joint damage areas concentrates at the top flange and corners of the joint. These denote the region where increased reliability needs strengthening. This correlates well with the results obtained by Libot et al. (2018) [51] who investigated the experimental strain energy density dissipated in SAC305 solder joints during different thermal cycling conditions using strain gauges measurements.

Ramachandran & Chiang (2017) [35] studied the feasibility evaluation of the creep model for failure assessment of solder joint reliability of wafer-level packaging. The simulation results of their research demonstrate that the maximum creep strain concentration happened in the corner of the solder joint near the chip pad side, which has a good agreement with the scanning electron microscope (SEM) image of solder joint crack location after failure from their simulated and experimental result. The Image of crack that was developed from the solder side near the silicon die at the point of the highest calculated strain observed. This shows that the stress/deformation occurs near the substrate as seen from the results of our simulation. Similarly, results obtained by Pierce et al. (2007) [52] shows similar results with high strain regions in the critical solder ball determined with FEM analysis and observation of the thermo-mechanical fatigue crack localised in the solder bulk on the component side.

2) Strain rate simulation results of solder joint subjected to thermal cycling

One of the significant results in this research is that solder joints failure is highly strained rate dependent. At higher strain rate, solder joint failed at much on the BGAs. Tsai et al. (2006) [64] investigated the high strain rate testing of solder interconnections. Their research shows that peak loads obtained from the impact tests are between 30% and 100% higher than those obtained from static shear tests for all combinations of solder alloy and pad finish. The plot obtained is presented in Fig. 10 with the strain rate schematic of this research shown in Fig. 11-14 showing areas with high strain rates. It could be seen that the strain rate represents

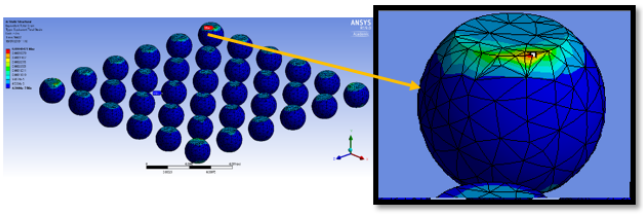

Fig. 11. **E**quivalent total strain for lead-based eutectic solder subjected to thermal cycling

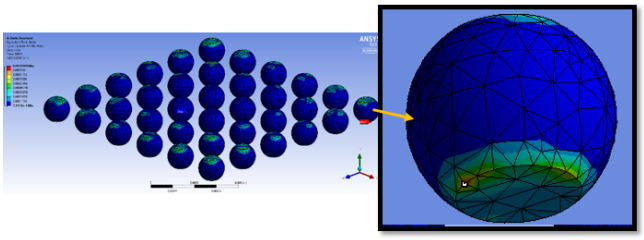

Fig. 12. **E**quivalent total strain for SAC305 solder subjected to thermal cycling

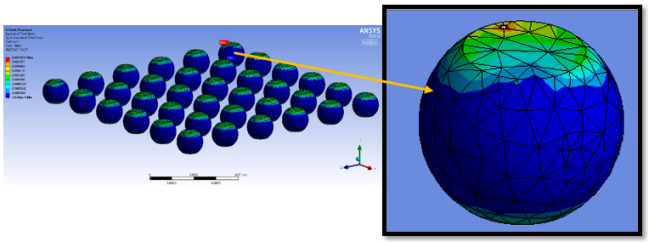

Fig. 13. **E**quivalent total strain for SAC387 solder subjected to thermal cycling

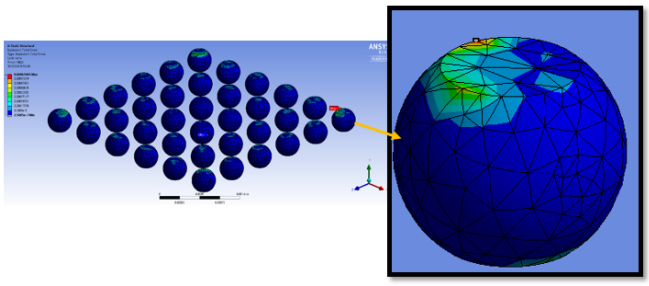

Fig. 14. **E**quivalent total strain for SAC396 solder subjected to thermal cycling

the quasi-static regime, and the strain is near top and the bottom of the BGA and PCB. The strain rate appears to be highest on SAC387 and lowest on the lead-based eutectic solder followed by SAC396 solder. It is expected that the solder joint is likely to fail under high strain rate load under different conditions including ageing time, strain and solder thickness.

VI. CONCLUSIONS

This research investigated the creep response of various solders used in soldering ball grid array (BGA) on printed circuit board (PCB) to find a suitable replacement for lead-based eutectic solder amidst increasing miniaturisation, function and thermo-mechanical reliability.

It is discovered that the distribution of damage in the BGA solder bump is at the top and bottom of the bumped joint.

Further findings reveal that the solder bumped joints at the periphery of the BGA accumulated more damage. The lead-free SAC396 is found to possess the least strain rate and strain energy damage than the lead-based eutectic solder. Based on the results, it is recommended that the lead-free SAC396 is the best replacement of the eutectic lead-based solder in the drive for the achievement of comparable thermo-mechanical reliability of assembled BGA on PCB.

VII. Acknowledgement

The authors thankfully acknowledge the funding contributions of the University of Derby.

References

[1] Kanlayasiri, K. and Sukpimai, K., 2016. Effects of indium on the intermetallic layer between low-Ag SAC0307-xIn lead-free solders and Cu substrate. Journal of Alloys and Compounds, 668, pp.169-175.

[2] Zhang, L. and Tu, K.N., 2014. Structure and properties of lead-free solders bearing micro and nano particles. Materials Science and Engineering: R: Reports, 82, pp.1-32.

[3] Coyle, R.J., Sweatman, K. and Arfaei, B., 2015. Thermal fatigue evaluation of Pb-free solder joints: results, lessons learned, and future trends. JOM, 67(10), pp.2394-2415.

[4] Schueller, R., Blattau, N., Arnold, J. and Hillman, C., 2010. Second generation Pb-free alloys. SMTA Journal, 23(1), pp.18-26.

[5] Plumbridge, W.J., 2005. Second generation lead-free solder alloysa challenge to thermodynamics. Monatshefte fr Chemie/Chemical Monthly, 136(11), pp.1811-1821.

[6] Ji, F., Xue, S., Zhang, L., Gao, L., Sheng, Z. and Dai, W., 2011. Reliability evaluation of QFN devices soldered joints with creep model. CHINESE JOURNAL OF MECHANICAL ENGINEERING-ENGLISH EDITION-, 24(3), pp.428-432.

[7] Sun, L., Zhang, L., Zhong, S.J., Ma, J. and Bao, L., 2015. Reliability study of industry Sn3. 0Ag0. 5Cu/Cu lead-free soldered joints in electronic packaging. Journal of Materials Science: Materials in Electronics, 26(11), pp.9164-9170.

[8] Zhang, Y., Cai, Z., Suhling, J.C., Lall, P. and Bozack, M.J., 2008, May. The effects of aging temperature on SAC solder joint material behavior and reliability. In 2008 58th Electronic Components and Technology Conference (pp. 99-112). IEEE.

[9] Zhang, J., Hai, Z., Thirugnanasambandam, S., Evans, J.L., Bozack, M.J., Sesek, R., Zhang, Y. and Suhling, J.C., 2012. Correlation of aging effects on creep rate and reliability in lead free solder joints. SMTA Journal, 25(3), pp.19-28.

[10] Hwang, J.S. and Vargas, R.M., 1990. Solder joint reliabilityCan solder creep?. Soldering & Surface Mount Technology, 2(2), pp.38-45.

[11] Huang, C., Yang, D., Wu, B., Liang, L. and Yang, Y., 2012, August. Failure mode of SAC305 lead-free solder joint under thermal stress. In 2012 13th International Conference on Electronic Packaging Technology & High Density Packaging (pp. 1395-1398). IEEE.

[12] Basaran, C., Ye, H., Hopkins, D.C., Frear, D. and Lin, J.K., 2005. Failure modes of flip chip solder joints under high electric current density. Journal of Electronic Packaging, 127(2), pp.157-163.

[13] Gomez, J. and Basaran, C., 2006. Damage mechanics constitutive model for Pb/Sn solder joints incorporating nonlinear kinematic hardening and rate dependent effects using a return mapping integration algorithm. Mechanics of Materials, 38(7), pp.585-598.

[14] Ghorbani, H.R. and Spelt, J.K., 2007. An analytical elasto-creep model of solder joints in leadless chip resistors: part 2applications in fatigue reliability predictions for SnPb and lead-free solders. IEEE Transactions on Advanced Packaging, 30(4), pp.695-704.

[15] Fahim, A., Ahmed, S., Chowdhury, M.R., Suhling, J.C. and Lall, P., 2016, May. High temperature creep response of lead free solders. In 2016 15th IEEE Intersociety Conference on Thermal and Thermomechanical Phenomena in Electronic Systems (ITherm) (pp. 1218-1224). IEEE.

[16] Ma, H., Suhling, J.C., Lall, P. and Bozack, M.J., 2006, May. Reliability of the aging lead free solder joint. In 56th Electronic Components and Technology Conference 2006 (pp. 16-pp). IEEE.

[17] Ma, H., Suhling, J.C., Zhang, Y., Lall, P. and Bozack, M.J., 2007, May. The influence of elevated temperature aging on reliability of lead free solder joints. In 2007 Proceedings 57th Electronic Components and Technology Conference (pp. 653-668). IEEE.

[18] Zhang, Y., Cai, Z., Suhling, J.C., Lall, P. and Bozack, M.J., 2009, May. The effects of SAC alloy composition on aging resistance and reliability. In 2009 59th Electronic Components and Technology Conference (pp. 370-389). IEEE.

[19] Zhang, Y., Cai, Z., Suhling, J.C., Lall, P. and Bozack, M.J., 2008, May. The effects of aging temperature on SAC solder joint material behavior and reliability. In 2008 58th Electronic Components and Technology Conference (pp. 99-112). IEEE.

[20] Cai, Z., Zhang, Y., Suhling, J.C., Lall, P., Johnson, R.W. and Bozack, M.J., 2010, June. Reduction of lead free solder aging effects using doped SAC alloys. In 2010 Proceedings 60th Electronic Components and Technology Conference (ECTC) (pp. 1493-1511). IEEE.

[21] Zhang, J., Hai, Z., Thirugnanasambandam, S., Evans, J.L., Bozack, M.J., Zhang, Y. and Suhling, J.C., 2013. Thermal aging effects on the thermal cycling reliability of lead-free fine pitch packages. IEEE transactions on components, packaging and manufacturing technology, 3(8), pp.1348-1357.

[22] Zhu, Y., Li, X., Wang, C. and Gao, R., 2015. A new creepfatigue life model of lead-free solder joint. Microelectronics Reliability, 55(7), pp.1097-1100.

[23] Amalu, E.H. and Ekere, N.N., 2016. Modelling evaluation of Garofalo-Arrhenius creep relation for lead-free solder joints in surface mount electronic component assemblies. Journal of Manufacturing Systems, 39, pp.9-23.

[24] Cadek, J., 1988. Creep in metallic materials.

[25] Ma, H. and Suhling, J.C., 2009. A review of mechanical properties of lead-free solders for electronic packaging. Journal of materials science, 44(5), pp.1141-1158.

[26] Otiaba, K.C., Bhatti, R.S., Ekere, N.N., Mallik, S. and Ekpu, M., 2013. Finite element analysis of the effect of silver content for SnAgCu alloy compositions on thermal cycling reliability of solder die attach. Engineering Failure Analysis, 28, pp.192-207.

[27] Terashima, S., Kariya, Y., Hosoi, T. and Tanaka, M., 2003. Effect of silver content on thermal fatigue life of Sn-xAg-0.5 Cu flip-chip interconnects. Journal of Electronic Materials, 32(12), pp.1527-1533.

[28] Ramachandran, V., Wu, K.C. and Chiang, K.N., 2018. Overview Study of Solder Joint Reliablity due to Creep Deformation. Journal of Mechanics, 34(5), pp.637-643.

[29] Chen, G., Zhao, X. and Wu, H., 2017. A critical review of constitutive models for solders in electronic packaging. Advances in Mechanical Engineering, 9(8), p.1687814017714976.

[30] Akbari, S., Lvberg, A., Tegehall, P.E., Brinkfeldt, K. and Andersson, D., 2019. Effect of PCB cracks on thermal cycling reliability of passive microelectronic components with single-grained solder joints. Microelectronics Reliability, 93, pp.61-71.

[31] Lau, J., Danksher, W. and Vianco, P., 2003, May. Acceleration models, constitutive equations, and reliability of lead-free solders and joints. In 53rd Electronic Components and Technology Conference, 2003. Proceedings. (pp. 229-236). IEEE.

[32] Pang, J.H., Low, T.H., Xiong, B.S., Luhua, X. and Neo, C.C., 2004. Thermal cycling aging effects on SnAgCu solder joint microstructure, IMC and strength. Thin solid films, 462, pp.370-375.

[33] Schubert, A., Dudek, R., Auerswald, E., Gollbardt, A., Michel, B. and Reichl, H., 2003, May. Fatigue life models for SnAgCu and SnPb solder joints evaluated by experiments and simulation. In 53rd Electronic Components and Technology Conference, 2003. Proceedings. (pp. 603-610). IEEE.

[34] Zhang, J., Hai, Z., Thirugnanasambandam, S., Evans, J.L., Bozack, M.J., Zhang, Y. and Suhling, J.C., 2013. Thermal aging effects on the thermal cycling reliability of lead-free fine pitch packages. IEEE transactions on components, packaging and manufacturing technology, 3(8), pp.1348-1357.

[35] Ramachandran, V. and Chiang, K.N., 2017. Feasibility Evaluation of Creep Model for Failure Assessment of Solder Joint Reliability of Wafer-Level Packaging. IEEE Transactions on Device and Materials Reliability, 17(4), pp.672-677.

[36] Pang, J.H., Xiong, B.S., Neo, C.C., Mang, X.R. and Low, T.H., 2003, May. Bulk solder and solder joint properties for lead free 95.5 Sn-3.8 Ag-0.7 Cu solder alloy. In 53rd Electronic Components and Technology Conference, 2003. Proceedings. (pp. 673-679). IEEE.

[37] Mukherjee, A.K., Bird, J.E. and Dorn, J.E., 1968. Experimental correlations for high-temperature creep.

[38] Garofalo, F., 1965. Fundamentals of creep and creep-rupture in metals(Creep and creep rupture in metals and alloys, fundamental information for instruction and reference). New York, Macmillan Co., Collier- Macmillan Ltd., 1965. 258 P.

[39] TopLine, 2016. TopLine. [Online] Available at: https://www.topline.tv/drawings/PDF/BGA

[40] JEDEC, 2009. Temperature cycling: JESD22-A104D, s.l.: JEDEC solid state technology association

[41] ESPEC, 2017. Temperature Cycling Chambers (Global-N Series), Mi, USA: ESPEC North America, Inc
[42] Almit Ltd, 2005. JEITA recommended. [Online] Available at: http://www.almit.com/dloads/Agents/SAC
[43] Ma, H., Suhling, J.C., Lall, P. and Bozack, M.J., 2006, May. Reliability of the aging lead free solder joint. In 56th Electronic Components and Technology Conference 2006 (pp. 16-pp). IEEE.
[44] Ma, H., Suhling, J.C., Zhang, Y., Lall, P. and Bozack, M.J., 2007, May. The influence of elevated temperature aging on reliability of lead free solder joints. In 2007 Proceedings 57th Electronic Components and Technology Conference (pp. 653-668). IEEE.
[45] Wiese, S., Schubert, A., Walter, H., Dukek, R., Feustel, F., Meusel, E. and Michel, B., 2001. Constitutive behaviour of lead-free solders vs. lead-containing solders-experiments on bulk specimens and flip-chip joints. In 2001 Proceedings. 51st Electronic Components and Technology Conference (Cat. No. 01CH37220) (pp. 890-902). IEEE.
[46] Vianco, P.T., 2005. Fatigue and creep of lead-free solder alloys: Fundamental properties. ASM International, pp.67-106.
[47] Wang, Q., Johnson, W., Ma, H., Gale, W.F. and Lindahl, D., 2005. Properties of lead free solder alloys as a function of composition variation. In 10th Electronic Circuit and World Convention Conference (ECWC 10).
[48] Sabbah, W., Bondue, P., Avino-Salvado, O., Buttay, C., Frmont, H., Gudon-Gracia, A. and Morel, H., 2017. High temperature ageing of microelectronics assemblies with SAC solder joints. Microelectronics Reliability, 76, pp.362-367.
[49] Pan, T.Y., 1994. Critical accumulated strain energy (case) failure criterion for thermal cycling fatigue of solder joints. Journal of electronic packaging, 116(3), pp.163-170.
[50] Dasgupta, A. and Oyan, C., 1991. Inelastic Strain Analysis of Solder Joint in NASA Fatigue Specimen.
[51] Fu, N., Ahmed, S., Suhling, J.C. and Lall, P., 2017, May. Visualization of Microstructural Evolution in Lead Free Solders During Isothermal Aging Using Time-Lapse Imagery. In 2017 IEEE 67th Electronic Components and Technology Conference (ECTC) (pp. 429-440). IEEE.
[52] Pierce, D.M., Sheppard, S.D., Vianco, P.T., Regent, J.A. and Grazier, J.M., 2007. Fatigue Life Prediction Methodology for Lead-Free Solder Alloy Interconnects: Development and Validation. In Proceedings of the IPC/JEDEC Global Conference on Lead Free Reliability & Reliability Testing for RoHS Lead Free Electronics (pp. 1-20).
[53] Lee, W.W., Nguyen, L.T. and Selvaduray, G.S., 2000. Solder joint fatigue models: review and applicability to chip scale packages. Microelectronics reliability, 40(2), pp.231-244.
[54] Gektin, V., Bar-Cohen, A. and Ames, J., 1997. Coffin-Manson fatigue model of underfilled flip-chips. IEEE Transactions on Components, Packaging, and Manufacturing Technology: Part A, 20(3), pp.317-326.
[55] Knecht, S. and Fox, L.R., 1990. Constitutive relation and creep-fatigue life model for eutectic tin-lead solder. IEEE Transactions on Components, Hybrids, and Manufacturing Technology, 13(2), pp.424-433.
[56] Dasgupta, A., 1993. Failure mechanism models for cyclic fatigue. IEEE Transactions on Reliability, 42(4), pp.548-555.
[57] Libot, J.B., Dulondel, F., Milesi, P., Alexis, J., Arnaud, L. and Dalverny, O., 2018, May. Experimental strain energy density dissipated in SAC305 solder joints during different thermal cycling conditions using strain gages measurements. In 2018 IEEE 68th Electronic Components and Technology Conference (ECTC) (pp. 748-755). IEEE.
[58] Darveaux, R. and Banerji, K., 1992. Constitutive relations for tin-based solder joints. IEEE Transactions on Components, Hybrids, and Manufacturing Technology, 15(6), pp.1013-1024.
[59] Otiaba, K.C., 2013. Thermal and thermo-mechanical performance of voided lead-free solder thermal interface materials for chip-scale packaged power device (Doctoral dissertation, University of Greenwich).
[60] Perkins, A. and Sitaraman, S.K., 2007. Universal fatigue life prediction equation for ceramic ball grid array (CBGA) packages. Microelectronics Reliability, 47(12), pp.2260-2274.
[61] Perkins, A., Tunga, K. and Sitaraman, S., 2006. Acceleration factor to relate thermal cycles to power cycles for ceramic ball grid area array packages. Journal of Microelectronics and Electronic Packaging, 3(4), pp.177-193.
[62] Zhang, L., Xue, S.B., Gao, L.L., Guang, Z.E.N.G., Yan, C.H.E.N., Yu, S.L. and Sheng, Z., 2010. Creep behavior of SnAgCu solders with rare earth Ce doping. Transactions of Nonferrous Metals Society of China, 20(3), pp.412-417.
[63] Zhang, L., Xue, S.B., Gao, L.L., Sheng, Z., Zeng, G., Chen, Y. and Yu, S.L., 2010. Properties of SnAgCu/SnAgCuCe soldered joints for electronic packaging. Journal of Materials Science: Materials in Electronics, 21(6), pp.635-642.
[64] Tsai, K.T., Liu, F.L., Wong, E.H. and Rajoo, R., 2006. High strain rate testing of solder interconnections. Soldering & surface mount technology, 18(2), pp.12-17.
[65] Zahn, B., 2002. Impact of ball via configurations on solder joint reliability in tape-based, chip-scale packages. San Diego, CA, USA, IEEE, pp. 1475-1483.
[66] T.Nguyen, T., Lee, D., B.Kwak, J. & Park, S., 2010. Effect of glue on reliability of flip chip BGA packages under thermal cycling. Microelectronics Reliability, July, 50(7), pp. 1000-1006.
[67] Long, X. et al., 2018. Constitutive behaviour and life evaluation of solder joint under the multi-field loadings. AIP Advances, 01 August, 8(8), pp. 085001-12.
[68] Beyer, H., Sivasubramaniam, V., Bayer, M. & Hartmann, S., 2016. Reliability of Lead-free Large Area Solder Joints in IGBT Modules with Respect to Passive and Active Thermal Cycling. Nuremberg, Germany, IEEE, pp. 1-6.
[69] Eckermann, J., Mehmood, S., Davies, H.M., Lavery, N.P., Brown, S.G.R., Sienz, J., Jones, A. and Sommerfeld, P., 2014. Computational modelling of creep-based fatigue as a means of selecting lead-free solder alloys. Microelectronics Reliability, 54(6-7), pp.1235-1242.
[70] Stoyanov, S., Bailey, C. and Desmulliez, M., 2009. Optimisation modelling for thermal fatigue reliability of lead-free interconnects in fine-pitch flip-chip packaging. Soldering & Surface Mount Technology, 21(1), pp.11-24.
[71] Amalu, E. H.& Ekere, N. N., 2016. Modelling evaluation of Garofalo-Arrhenius creep relation for lead-free solder joints in surface mount electronic component assemblies. Journal of Manufacturing Systems, April, Volume 39, pp. 9-23.